Thermal performance of inserting hybrid nanofluid in parabolic trough collector

Otabeh Al-Oran* and Ferenc Lezsovits

Department of Energy Engineering, Faculty of Mechanical Engineering, Budapest University of Technology and Economics, Műegyetem rkp. 3, 1111 Budapest, Hungary

AKADÉMIAI KIADÓ

Pollack Periodica • An International Journal for Engineering and Information Sciences

16 (2021) 3, 88–93

DOI: 10.1556/606.2021.00318

Received: December 17, 2020 • Revised manuscript received: January 5, 2021 • Accepted: January 9, 2021
Published online: April 21, 2021

ORIGINAL RESEARCH PAPER

ABSTRACT

In this work, the thermal performance of using hybrid nanofluid of Ceria oxide and multi-walled carbon nanotube-based MOL 68 in the receiver tube of parabolic trough collector is simulated numerically. The influence of using this nanofluid under various volume concentrations and different Reynold numbers is solved numerically using computational fluid dynamics. The turbulent model's analysis is carried out based on k–ε re-normalization group and employed to find the Nusselt number and the heat transfer coefficients. The model results were validated with the previous correlation, which were used to evaluate the Nusselt number. The results showed that hybrid nanofluid enhances the heat transfer characteristics of the parabolic trough collector in comparison with the base fluid. Furthermore, even better heat transfer characteristics can be achieved with an increased volume concentration of the modified nanofluids.

KEYWORDS

hybrid nanofluids, numerical study, Nusselt number, heat transfer coefficients, parabolic trough collector

1. INTRODUCTION

Recently, there has been increasing attention to using clean and renewable energy and its applications. This attention is due to the expanding rate of electricity prices, the decrease in fossil fuel levels worldwide, and increased demand as a result to the growing population, side by side with environmental problems [1]. Solar energy is considered as the most widely used and the most important compared to other types of clean energy. This is due to its availability and ability to synchronize with different applications at an acceptable financial cost [2, 3]. Using the Parabolic Trough Collector (PTC) as an application for concentrated solar energy It is beginning to spread because of its ability to produce electricity, besides to its ability to produce medium and high temperatures. Therfore, this type is most applicable to be used in different applications, like heating, desalination, produce electricity, and refrigeration [4]. On this basis various studies have been done to enhance the heat transfer of the receiver tube for the PTC. This enhancement can be reached using various methods, namely passive, active techniques or combined both methods [5]. One of the most recent ways that have taken a broad interest in recent years is the use of nanofluid that is clearly shown by an increase in the number of articles in this field [6]. This method is based on improving the thermal properties of the base fluid by adding small nanoparticles on the base fluid, which leads to enhance thermal properties, especially thermal conductivity of the modified fluid, which reflected on improving the performance of the whole system [7]. Olia et al. [8] in their review, were summarized the effect of inserting various mono nanoparticles types in different base fluids, whether the results obtained from numerically using various software or experimentally. The high accuracy of utilizing Computational Fluid Dynamic (CFD) tool side by side with the ability to describe detailed components like: fluid flow and the heat flux profiles, supports to use this software on a wide range to describe the nanofluid effect on the thermal performance. So different studies were performed using CFD tools to examine many mono

*Corresponding author.
E-mail: aloran@energia.bme.hu

AKJournals

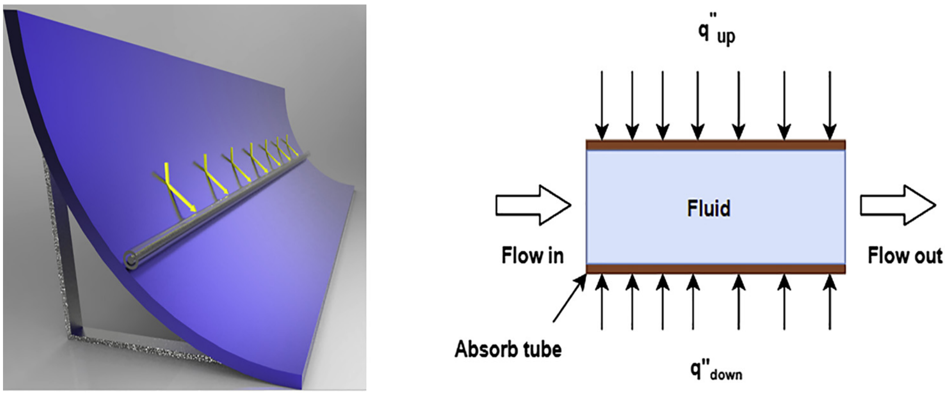

Fig. 1. Conceptual PTC and receiver tube description

nanofluids like using Al_2O_3 based Therminol 66 [9], where in this study the researchers presumed that the receiver tube affected by different heat flux as a boundary condition applied on the upper and lower sides. On the other hand, some researchers [10] linked the exact heat flux achieved using ray tracing with the CFD tools to evaluate and describe the effect of inserting mono nanofluids on the thermal performance of PTC. The positive results of nanofluid use have prompted researchers to improve this method's use by merging more than one nanoparticle (hybrid nanofluid) to achieve better thermal performance with acceptable cost. However, so far, only a few research has used the influence of utilizing hybrid nanofluid in the PTC solar application [11]. Ekiciler et al. [12] in their research, developed and compared the effect of inserting three hybrid nanofluid types (Ag–ZnO, Ag–MgO, and Ag–TiO_2) based Syltherm 800 numerically using CFD software. The major results present thermal efficiency enhancement reaches 15% using Ag–MgO/Syltherm 800 under high concentrations.

As it can be seen in the previous section, researches on the effect of using hybrid nanofluid in the PTC did not take a high interest in comparison with mono nanofluid. This study aims to examine the thermal performance of PTC with hybrid nanofluid under turbulent flow conditions for the constant temperature of 100 °C. The numerical simulation is obtained by using computational fluid dynamics. Also, the effect of inserting different nanoparticle volume concentrations on hydraulic and heat transfer performances is investigated.

2. MODEL SPECIFICATION AND METHODOLOGY

The problem statement of the present work is based on solving the governing equations (momentum, energy, and continuity) in three-dimensional of the Hybrid NanoFluid (HNF) under turbulent flow and variable heat flux conditions as shown in Eqs (1)–(6), where the schematic descriptions of the PTC and their receiver tube that affected by different heat flux on both sides are presented in Fig. 1. In details, the receiver tube specifications and the heat flux conditions that applied on both sides are tabled as shown in Table 1.

Continuity equation:

$$\nabla.\left(\rho_{hnf} V\right) = 0, \tag{1}$$

where the V describes velocity in (R, θ, Z).

Momentum equation:

$$\nabla.\left(\rho_{hnf} V V_i\right) = \frac{\partial p}{\partial X_i} + \nabla.\left(\mu_{hnf} \nabla V_i\right) + S_i, \tag{2}$$

where $x_i = (R, \theta, Z)$ for spatial direction, while S_i present the remaining viscose terms and its derived in three directions as follows:

$$S_R = \rho_{hnf} V_\theta \frac{V_\theta}{R} - \mu_{hnf}\left[\frac{V_R}{R^2} + \frac{2}{R^2}\frac{V_\theta}{\partial\theta}\right], \tag{3}$$

$$S_\theta = -\rho_{hnf} V_R \frac{V_\theta}{R} + \mu_{hnf}\left[\frac{-V_\theta}{R^2} + \frac{2}{R^2}\frac{V_R}{\partial\theta}\right], \tag{4}$$

$$S_Z = 0. \tag{5}$$

Finally, the energy equation holds:

$$\nabla.\left(\rho_{hnf} V C_{P,hnf} T\right) = \nabla.\left(k_{hnf} \nabla T\right). \tag{6}$$

2.1. Hybrid nanofluid

In this study, nanofluid of mixing MOL 68 (Hungarian oil) at constant temperature of 100 °C and hybrid nanoparticles of Multi-Walled Carbon NanoTube-CeO_2 (MWCNT-CeO_2) under volume fraction 50:50 is considered as a thermal

Table 1. Technical specification of receiver tube and heat flux boundary conditions

Parameter [Symbols]	Specifications
Receiver length [L]	2 m
Receiver inner diameter [$d_{R,i}$]	0.066 m
Receiver outer diameter [$d_{R,o}$]	0.07 M
Concentrated ratio [C_R]	30
Receiver material	Steel
Upper heat flux [q''_{up}]	750 W/m^2
lower heat flux [q''_{down}]	19,500 W/m^2

Table 2. Base fluid and nanoparticles thermal properties [11, 15]

Property	Unit	MWCNT	CeO_2	HNP	MOL 68
Specific heat (C_p)	J/kg K	710	460	585	2,160
Density (ρ)	kg/m^3	2,100	7,220	4,660	828
Thermal conductivity (k)	W/m K	2,000	12	1,006	0.126
dynamic viscosity (μ)	Pa. s	–	–	–	0.0072

heating fluid. The following equations of classical models are utilized to describe thermal properties of the modified nanofluid, where those equations results are justified and widely used in literature [13, 14]. Furthermore, the main thermal properties of MOL 68 and nanoparticles are presented as shown in Table 2 [11, 15].

The total volume concentration of the combination that obtained by inserting MWCNT and CeO_2 was defined as represented in Eq. (7) [13]. To simplify equation MWCNT, CeO_2 subscribed by n_{p1} and n_{p2}, and φ, respectively, where thermal performance was examined under different total volume fraction φ_{tot} varied 0–4%,

$$\varphi_{tot} = \varphi_{np1} + \varphi_{np2}. \tag{7}$$

Equation (8) expresses hybrid nanofluid density in kg/m^3, where, base fluid subscribed by b_f while modified hybrid nanofluid subscribed by *hnf* [11],

$$\rho_{hnf} = \varphi_{np1}.\rho_{np1} + \varphi_{np2}.\rho_{np2} + (1-\varphi_{tot}).\rho_{bf}. \tag{8}$$

Specific heat capacity in J/kg·K formula represented in Eq. (9) was used widely in literature; related to its ability to cover a wide range of the volume concentration,

$$C_{p,hnf} = \frac{\varphi_{np1}.\rho_{np1}.C_{p,\ np1} + \varphi_{np2}.\rho_{np2}.C_{p,\ np2}}{\rho_{hnf}} + \frac{(1-\varphi_{tot}).\rho_{bf}.C_{p,\ bf}}{\rho_{hnf}}. \tag{9}$$

The thermal conductivity of the nanofluid was obtained using Maxwell correlation as it is shown in Eq. (10) to obtain the hybrid nanofluid thermal conductivity in W/m·K,

$$V_1 = \frac{\varphi_{np1}.\,k_{np1} + \varphi_{np2}.\,k_{np2}}{\varphi_{tot}},$$
$$V_2 = \varphi_{np1}.\,k_{np1} + \varphi_{np2}.\,k_{np2}, \tag{10}$$
$$k_{hnf} = k_{bf}\left[\frac{V_1 + 2.\,k_{bf} + 2\cdot V_2 - 2\cdot\varphi_{tot}.k_{bf}}{V_1 + 2\cdot k_{bf} - V_2 + \varphi_{tot}.k_{bf}}\right].$$

Finally, the association of the Brinkman model was used to obtain the dynamic viscosity of the nanofluid as it is presented in Eq. (11),

$$\mu_{nf} = \mu_{bf}\frac{1}{(1-\varphi)^{2.5}}. \tag{11}$$

2.2. Numerical procedure and boundary conditions

In this section, the receiver tube geometrical of the present work is created and meshed using the CFD software

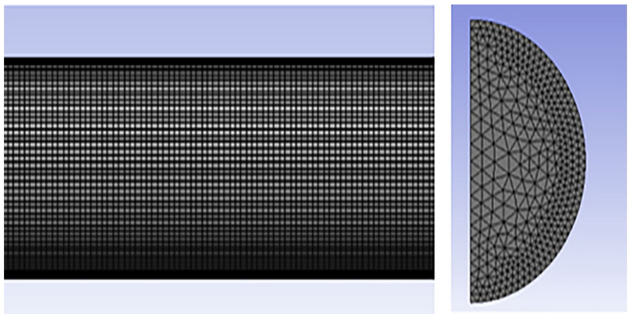

Fig. 2. Front and side views of the used mesh

presented in Fig. 2. This mesh is based on the defined mesh as a triangular mesh with a high focus on the susceptible area section, which is near the receiver wall. Actually, to optimize the time consuming to solve governing equations using the Finite Volume Method (FVM), only half of the tube has been considered; this is according to the symmetry about the vertical axis. Fluent in ANSES-2019R2 is used to describe and solve governing equations of steady-state turbulent flow inside the receiver tube of this work up to convergence 10^{-6}. The k–ε RNG model with standard wall function is adapted to define the turbulence of the base and nanofluids flow inside PTC receiver tube; this attributed to their sensitivity to describe the effect of the flow separation and rapid strain streamlines; side by side with the excellent prediction results obtained by using this model as it is mention by Ghasemi and Ranjbar in their research [16]. Finally, various boundary conditions are adapted to solve the problem; whereas those boundaries were summarized as follow:

- The uniform inlet velocity and the temperature is considered, where the velocity value obtained depends on the *Re* number values, while inlet temperature evaluated at T_{in}= 373 K.
- There are no-slip conditions inside the tube wall.
- The zero pressure gradient situation is used across the exit boundary.
- The uniform heat flux boundary conditions on both outer sides of the tube are defined as prescribed in Table 1.

3. RESULTS AND DISCUSSIONS

With the objective of minimizing the errors of the simulation, the test of grid independence for water as a base fluid in Fig. 3 occurred under various inlet velocities to cover the *Re* numbers ranged 30,000 up to 250,000. Those variations aimed to obtain the Nusselt number. In the following figure, the independence test occurred for the Nusselt number presented for the mesh elements numbers (75,835, 285,150, and 450,892 elements). The trend of all independence tests shows an increase in the *Nu* with the increase in *Re* number; besides, the significant results reported small variation between *Nu*'s increase, particularly between the second and

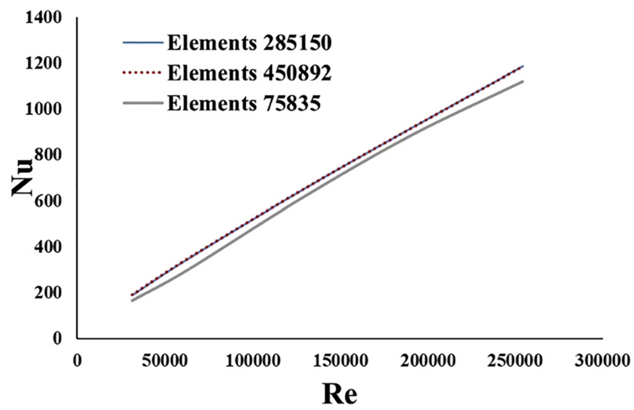

Fig. 3. Grid independence test for three grids number

third independence tests, which means convergence to the high-quality mesh. Accordingly, the independence test number two which has element number 285,150 is utilized in this research to evaluate the convective heat transfer coefficient of the modified thermal fluid. To be sure about the precision of the present model result, the numerical results of the dimensionless *Nu* number of the water were validated with different experimental correlations [17]; as it is presented in Fig. 4. These results tend to agree with all correlations reported in the literature. Besides, it strongly agreed with the *Nu* values obtained with Notter and Ross correlation compared with other correlations under average errors equal to 6.5%, which is acceptable in this application.

Figure 5 is used to present heat transfer coefficient variation against *Re* number for base fluid and HNFs concentrations. Whereas the increase of this coefficient is a result of the reflected obtained increase in *Nu* number with increasing *Re*; this attributed to the occurred increase in the turbulence of the fluid. Hint the surface report definition is used to obtain average local *Nu* number and heat transfer coefficient as it is shown in the following equations. In addition, it is evident in Fig. 5 the positive effect of increasing the concentrations in the heat transfer coefficient compared with the base fluid. In detail, the convection heat

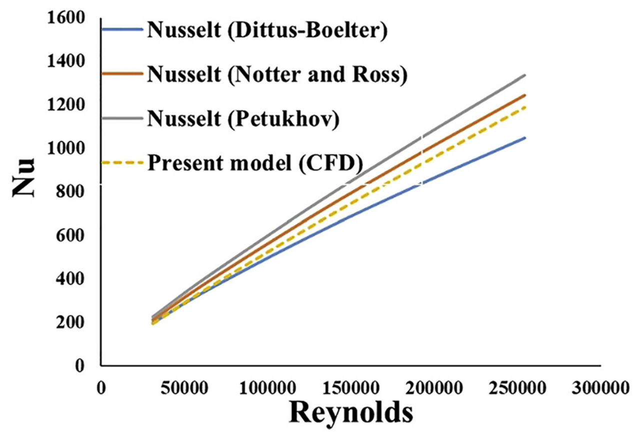

Fig. 4. Validation *Nu* number of present model with correlations under various *Re* number

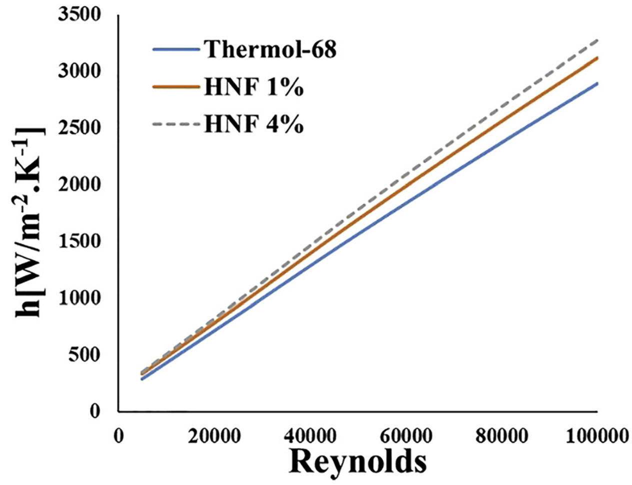

Fig. 5. Heat transfer coefficient versus Reynold number for different concentration volume

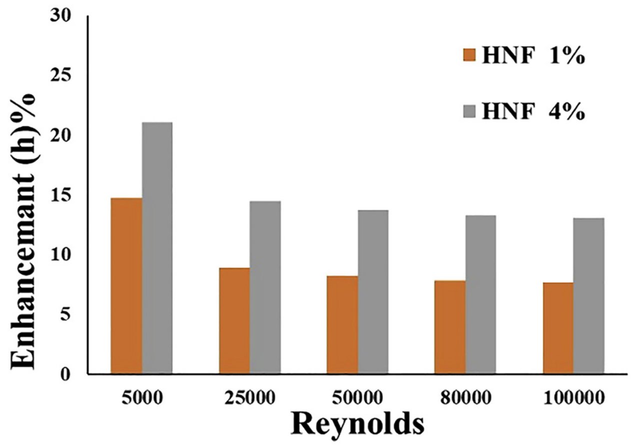

Fig. 6. Heat transfer coefficient enhancement versus Reynold number for different concentration volume

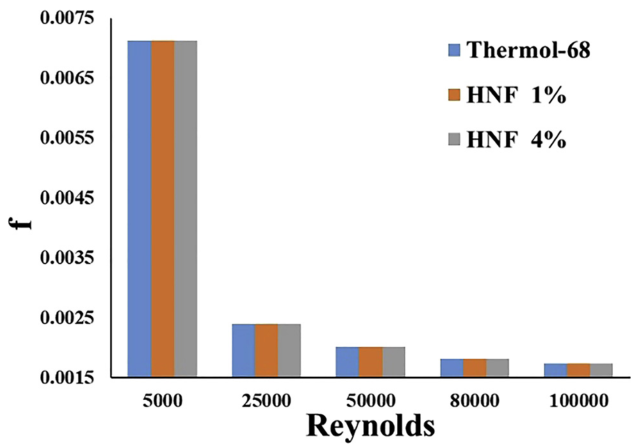

Fig. 7. Friction factor versus Reynold number for different concentration volume

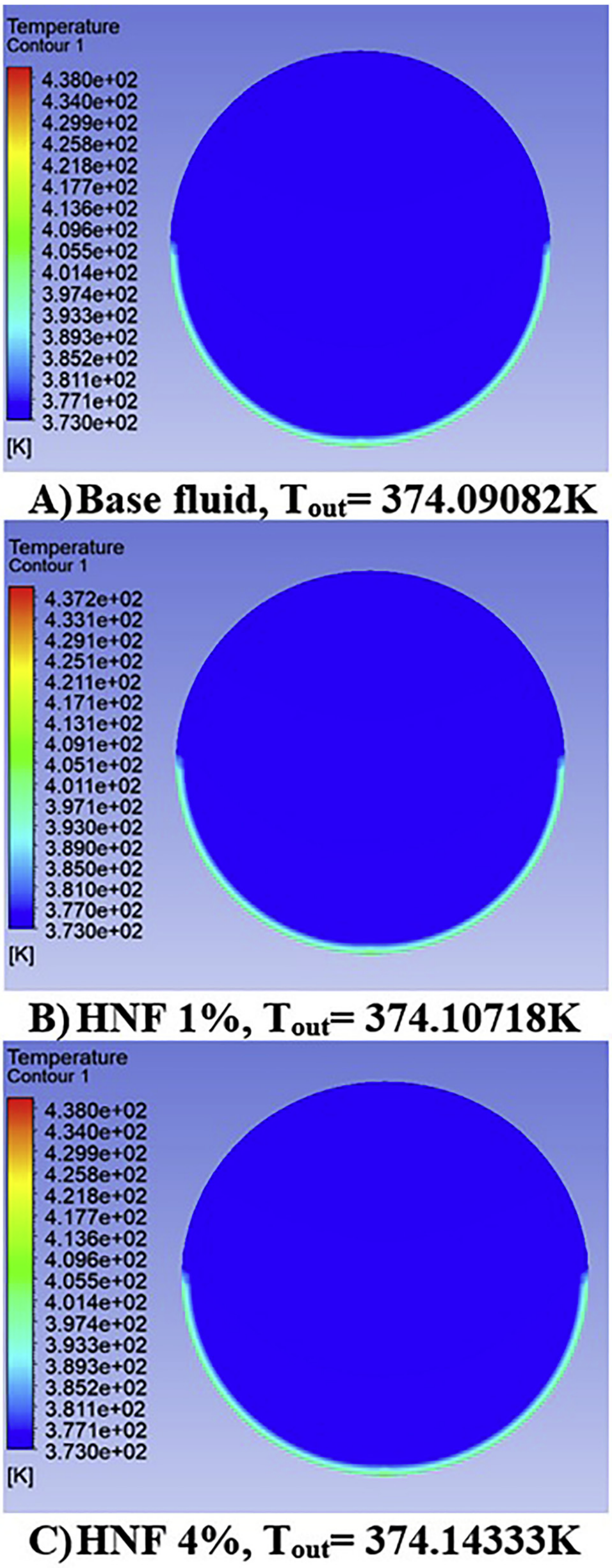

Fig. 8. Temperatures contours and outlet temperature of A) base fluid B) HNF 1% C) HNF 4%

transfer varied with *Re* number from low to high values as follows: 331.753 up to 3120.150 for concentration 1%, while it ranged from 350.05 up to 3276.54 for concentration 4%.

The Nusselt number is:

$$Nu = \frac{h_f D_{in}}{k_f}. \tag{12}$$

The heat transfer coefficient is:

$$h_f = \frac{q''}{T_{di} - T_{fm}}. \tag{13}$$

To clarify the enhancement impact of utilized nanofluid concentrations (Fig. 6) presents the enhancement ratio on heat transfer coefficient. The results show a high enhancement ratio of 21% obtained at a concentration of 4% and a low *Re* number. This can be justified by the enhancement of the increase in the thermal conductivity of the modified nanofluid.

For hydrodynamic performance (Fig. 7) express the variation of friction factor concerning with *Re* number for base fluid and hybrid nanofluid volume concentrations in the receiver, where the pressure drop difference (Δp) that evaluated from the fluent is used to calculate friction factor as it is shown in the Blasius Eq. (14),

$$f = \frac{2D\Delta p}{\rho u^2 L}. \tag{14}$$

It is clear from Fig. 7 that the friction factor of the base fluid and both HNF concentrations has the same inverse trend with the increase in *Re* numbers. This can be attributed to the inverse relationship between velocity and friction factor. The major results obtained in this figure fired unclear enhancement reached by increasing the nanoparticle concentrations consider positive results to use this HNFs combination.

Finally, the contour plot of the outlet temperature presented as it is observe in Fig. 8 for the base fluid and HNF concentrations at Reynold number 5×10^3. The results show low increase in the outlet temperature with the concentration increase this can be justified by the high velocity of the contour plot.

4. CONCLUSIONS

In this study, the convective heat transfer coefficient and hydrodynamic behaviors of utilizing hybrid nanofluid of multi-walled carbon nanotube and CeO_2/MOL68 were investigated numerically under various turbulent flows Reynolds numbers range (5×10^3–10×10^3) and concentrations volumes (0, 1, and 4%). The heat transfer coefficient results present a notable enhancement that increases by increasing concentrations where it showed enhancements reach of 14.77% by 1% *V* concentration and 21% by 4% *V* concentration. In addition, another positive goal achieved by the use of this hybrid nanofluid is that there is a slight increase in friction factor due to increased concentrations, which has a positive effect on the pumping force, required driving fluids.

REFERENCES

[1] O. Al-Oran and F. Lezsovits, "Enhance thermal efficiency of parabolic trough collector using Tungsten oxide/Syltherm 800 nanofluid," *Pollack Period.*, vol. 15, no. 2, pp. 187–198, 2020.

[2] L. Al-Ghussain, O. Al-Oran, and F. Lezsovits, "Statistical estimation of hourly diffuse radiation intensity of Budapest City," *Environ. Prog. Sustain. Energ.*, vol. 40, no. 1, 2021, Paper no. e13464.

[3] A. Caló and E. Pongrácz, "The role of smart energy networks to support the application of waste-to-energy technologies," *Pollack Period.*, vol. 9, Supplement 1, 2014, pp. 61–73.

[4] L. Evangelisti, R. D. L. Vollaro, and F. Asdrubali, "Latest advances on solar thermal collectors: A comprehensive review," *Renew. Sustain. Energ. Rev.*, vol. 114, Paper no. 109318, 2019.

[5] O. Al-Oran and F. Lezsovits, "Recent experimental enhancement techniques applied in the receiver part of the parabolic trough collector - A review," *Int. Rev. Appl. Sci. Eng.*, vol. 11, no 3, pp. 209–219, 2020.

[6] E. C. Okonkwo, I. Wole-Osho, I. W. Almanassra, Y. M. Abdullatif, and T. Al-Ansari, "An updated review of nanofluids in various heat transfer devices," *J. Therm. Anal. Calorim.*, pp. 1–56, 2020. doi.org/10.1007/s10973-020-09760-2.

[7] M. S. Kamel, O. Al-Oran, and F. Lezsovits, "Thermal conductivity of Al_2O_3 and CeO_2 nanoparticles and their hybrid based water nanofluids: An experimental study," *Periodica Polytech., Chem. Eng.*, vol. 65, no. 1, pp. 50–60, 2021.

[8] H. Olia, M. Torabi, M. Bahiraei, M. H. Ahmadi, M. Goodarzi, and M. R. Safaei, "Application of nanofluids in thermal performance enhancement of parabolic trough solar collector: state-of-the-art," *Appl. Sci.*, vol. 9, no. 3, pp. 1–22, 2019.

[9] S. E. Ghasemi and A. A. Ranjbar, "Effect of using nanofluids on efficiency of parabolic trough collectors in solar thermal electric power plants," *Int. J. Hydrogen Energ.*, vol. 42, no. 34, pp. 21626–21634, 2017.

[10] A. Mwesigye, Z. Huan, and J. P. Meyer, "Thermal performance and entropy generation analysis of a high concentration ratio parabolic trough solar collector with Cu-Therminol® VP-1 nanofluid," *Energ. Convers. Manage.,* vol. 120, pp. 449–465, 2016.

[11] O. Al-Oran, F. Lezsovits, and A. Aljawabrah, "Exergy and energy amelioration for parabolic trough collector using mono and hybrid nanofluids", *J. Therm. Anal. Calorim.*, vol. 40, pp. 1579–1596, 2020.

[12] R. Ekiciler, K. Arslan, O. Turgut, and B. Kurşun, "Effect of hybrid nanofluid on heat transfer performance of parabolic trough solar collector receiver," *J. Therm. Anal. Calorim.*, vol. 143, pp. 1637–1654, 2020.

[13] B. Takabi and S. Salehi, "Augmentation of the heat transfer performance of a sinusoidal corrugated enclosure by employing hybrid nanofluid," *Adv. Mech. Eng.*, vol. 6, 2014, Paper no. 147059.

[14] R. A. Rasih, N. A. C. Sidik, and S. Samion, "Recent progress on concentrating direct absorption solar collector using nanofluids," *J. Therm. Anal. Calorim.*, vol. 137, no. 3, pp. 903–922, 2019.

[15] S. Giwa, M. Sharifpur, and J. Meyer, "Experimental study of thermo-convection performance of hybrid nanofluids of Al_2O_3-MWCNT/water in a differentially heated square cavity," *Int. J. Heat Mass Transfer*, vol. 148, Paper no. 119072, 2020.

[16] S. E. Ghasemi and A. A. Ranjbar, "Effect of using nanofluids on efficiency of parabolic trough collectors in solar thermal electric power plants," *Int. J. Hydrogen Energ.*, vol. 42, no. 34, pp. 21626–21634, 2017.

[17] T. L. Bergman, F. P. Incropera, A. S. Lavine, and D. P. DeWitt, *Introduction to Heat Transfer*. John Wiley & Sons, 2011.